Latin American Journal of Solids and Structures
www.lajss.org

Near the resonance behavior of a periodicaly forced partially dissipative three-degrees-of-freedom mechanical system

Abstract
In this paper, a nonlinear three-degrees-of-freedom dynamical system consisting of a variable-length pendulum mass attached by a massless spring to the forced slider is investigated. Numerical solution is preceded by application of Euler-Lagrange equation. Various techniques like time histories, phase planes, Poincaré maps and resonance plots are used to observe and identify the system responses. The results show that the variable-length spring pendulum suspended from the periodically forced slider can exhibit quasi-periodic, and in a resonance state, even chaotic motions. It was concluded that near the resonance the influence of coupling of bodies on the system dynamics can lead to unpredictable dynamical behavior.

Keywords
Euler-Lagrange equation, time history, phase plane, Poincaré map, resonance plot, dynamical analysis, quasi-periodic motion, chaos.

Paweł Pietrzak[a]
Marta Ogińska[a]
Tadeusz Krasuski[a]
Kévin Figueiredo[a]
Paweł Olejnik[b*]

[a] International Faculty of Engineering, Lodz University of Technology, 36 Żwirki Str., 90-001 Lodz, Poland. E-mail: pawel-pietrzak@outlook.com, martaoginska93@gmail.com, krasuski.tadeusz@gmail.com, figueiredo.kevin@outlook.fr.

[b] Department of Automation, Biomechanics and Mechatronics, Faculty of Mechanical Engineering, Lodz University of Technology, 1/15 Stefanowski Str., 90-924 Lodz, Poland. E-mail: pawel.olejnik@p.lodz.pl.

*Corresponding author

http://dx.doi.org/10.1590/1679-78254423

Received August 23, 2017
In revised form December 19, 2017
Accepted December 19, 2017
Available online February 02, 2018

1 INTRODUCTION

The existence of the resonance phenomena both external and internal occurs in vibrating structures as an increased amplitude of vibrations. In general, from the engineering point of view, this type of grazing behavior is usually unwanted also in solid bodies. Appearance of resonance generate greater complexity of a mechanical system behavior (Nayfeh and Mook, 1979). In this paper, the study is performed to create the simulation and investigation for better understating of resonance phenomenon of a periodically forced slider-spring pendulum mechanical system of three degrees of freedom.

The first and the most important question to answer is what the resonance is from the point of view of mechanical engineering. It is a phenomenon describing the tendencies of a mechanical system to increase its amplitude when the external excitation force acts with certain fixed frequency. This frequency of periodic excitation needs to be close or exactly the same as the internal system's natural frequency (such frequency is called the resonance frequency). Such increased vibration amplitudes will only appear when the excitation is exactly the same or is a multiple of one of the natural frequencies of the system. This phenomenon can be destructive for structures and even solid bodies in its effects due to the fact that in certain range of parameters from the external excitation, the forces acting on the objects highly increase. The most commonly used example of not including and wrongly treated resonance phenomena is the collapse of Tacoma Narrows Bridge in 1940. The periodic vibration and rhythmic twisting leaded to destruction of the construction, not only due to simple mechanical resonance, but to a more complicated interaction between the bridge and the wind passing through it is a phenomenon called aeroelastic flutter discovered by Robert H. Scanlan. Flutter is a dynamic instability of an elastic structure in a fluid flow caused by positive feedback between the body's deflection and the force exerted by the fluid flow. Nevertheless, resonance

should not be treated as the side effect phenomenon in each case. For many devices, we are able to work more efficiently with less amount of input power. The positive side of resonance is generally used in vibrating tables for increasing their amplitude but also all the music instruments are in favor of acoustic resonance.

In this study a nonlinear dynamical system of three degrees of freedom with a spring pendulum (Zhang *et al.*, 2015; Plaksiy and Mikhlin, 2017) and a vibrating suspension (Aduyenko and Amel'kin, 2015) will be investigated, as it was similarly carried out in (Sado, 2003). The mechanical systems have a variety of applications in our daily life and they should be still investigated.

The pendulum may be suspended to the flexible element. In this system the autoparametric excitation may occur as a result of inertial coupling. Analogous behavior happens when the mass is attached to the pendulum type elastic oscillator, and then, it is possible to observe autoparametric nonlinear coupling between the angle of the pendulum and elongation of the spring. All of such cases depend on the set of parameters for the investigated system. Examples are as follows: dumping, mass ratio of components, and specification of external excitation. As a result of system specification, the resonance phenomenon transferring the energy between system components or their mutual excitation can appear differently.

According to Francis C. Moon, chaotic vibrations is a kind of a system behavior that despite the fact of using fast computers there is no infinite predictability in the observed dynamics. It is now known that the motion of very simple dynamical systems cannot always be predicted far into the future. Such motions have been labelled as chaotic (Moon, 1987).

For many studies of the three-degrees-of-freedom systems and chaotic behavior neither for the parametric or autoparametric excitation have been observed. In this paper, we investigate this area by performing both analytical and numerical solutions to describe the external and internal resonance behavior of such system.

The observations brings interesting results, summarizing that the mechanical system with partial dissipation of kinetic energy of motion oscillates mainly periodically and quasi-periodically. The system dynamics exhibits chaos in a close vicinity of resonance peaks of maximum amplitudes.

2 PROBLEM DESCRIPTION

We analyze the three-degrees-of-freedom dynamical system presented in Figure 1.

Our system consists of an elastic pendulum with the initial length l_0, the stiffness k and damping c. The pendulum is attached to the moving slider with the point-focused mass M. The slider moves horizontally along the x axis. The mass m hangs down from the end of the spring. The body of mass M (slider) is subjected to the harmonic vertical excitation force $F(t) = F_0 \cos\omega t$. The planar mechanical system presented above has three degrees of freedom (Hatwal *et al.*, 1983; Lynch, 2002; Rossikhin and Shitikova, 2006; Kartachov, 2016). The generalized coordinates are assumed for the angle θ between the pendulum spring and the vertical axis z (inclination angle), the incremental elongation of the spring Δs and the horizontal displacement x of the body of mass M.

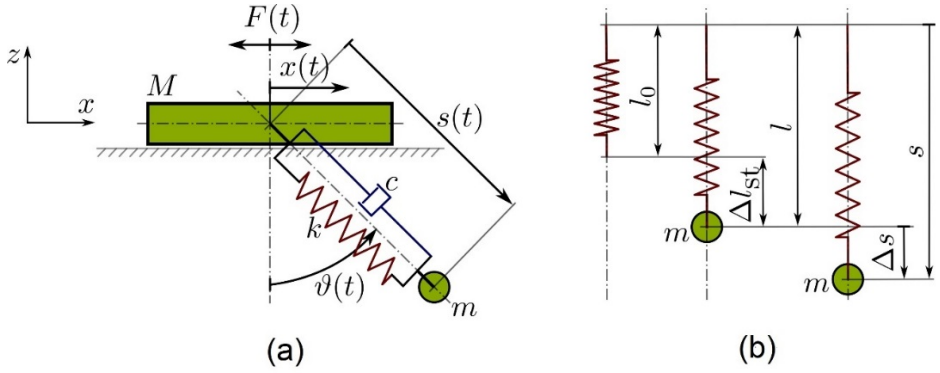

Figure 1: *A variable-length forced spring pendulum system of three degrees of freedom (a), and the dimensions of loaded (stretched or compressed) and unloaded (free) linear spring (b).*

Any of the existing phenomena cannot be presented, examined and transferred to mathematical or engineering problem in the infinitely direct way (Olejnik and Awrejcewicz, 2018). According to this fact, some assumptions allowing for a reduction of the complexity of the analyzed problem will be made. To weaken the system's complexity, but still maintaining its basic properties we assume that:

- friction of the slider does not exist in the dynamical system;
- energy dissipated by the frictional contact of the base and the slider vibrating on it can be compensated from an external source of energy, for instance, determined by a control system;
- radial elongation of the spring pendulum exists;
- the spring is considered as massless, and its force of reaction described by Hooke's law appears when it is stretched or compressed from its free length;
- the slider has a point mass focused at the rotationally constrained end (upper) of the spring;
- excitation is caused by an external harmonic force, e.g., it can come from a magnetic field;
- mass of the spring pendulum is focused in a point at the second (lower) end of the spring;
- damping of motion is associated only with elongation of the spring of the pendulum.

We assume the almost ideal case in which the dissipation of energy by the frictional contact could be partially compensated by an external source.

3 MATHEMATICAL MODELING

For the mathematical description of the dynamical system with a time-varying parameter, such as the variable length of the pendulum, the Hill or Mathieu equations are often used (Nayfeh and Mook, 1979). Nevertheless, in similar studies referring to the analyzed case, the Euler-Lagrange equation can be used (Srinivasan and Sankar, 1974).

The kinetic energy of the analyzed three-degrees-of-freedom system is calculated according to the sum of kinetic energies of both system bodies (see Figure 1):

$$\begin{aligned} U(\vartheta, s, x, \dot{\vartheta}, \dot{s}, \dot{x}) &= \frac{1}{2} M\dot{x}^2 + \frac{1}{2} m\left[\left(\dot{x} + \dot{s}\sin\vartheta + s\dot{\vartheta}\cos\vartheta\right)^2 + \left(s\dot{\vartheta}\sin\vartheta - \dot{s}\cos\vartheta\right)^2\right] \\ &= \frac{1}{2}\left(M + m\right)\dot{x}^2 + \frac{1}{2} m\left[\dot{s}^2 + s^2\dot{\vartheta}^2 + 2\dot{x}\left(\dot{s}\sin\vartheta + s\dot{\vartheta}\cos\vartheta\right)\right]. \end{aligned} \tag{1}$$

The potential energy of the analyzed mechanical system is a sum of a) the energy of the linear spring, that is accumulated after the incremental elongation Δs and the static elongation Δl_{st} (static stretching or compression by a hanging pendulum body of mass m, see Figure 1) measured from the equilibrium free length l_0 of the spring and b) the gravitational potential energy of the body of mass m on the vertical distance $(\Delta s + l)\cos\vartheta$ between centres of the slider and the pendulum body, i.e.,

$$V(\vartheta, \Delta s, x) = \frac{1}{2} k(\Delta s + \Delta l_{st})^2 - mg\left(\Delta s + l\right)\cos\vartheta. \tag{2}$$

Taking into account that

$$\Delta s + \Delta l_{st} = s - l_0, \quad l = l_0 + \Delta l_{st}, \tag{3}$$

one finds

$$V(\vartheta, s, x) = \frac{1}{2} k(s - l_0)^2 - mgs\cos\vartheta. \tag{4}$$

At independence of the assumed generalized coordinates y_k, the Lagrangian $L = U - V$ satisfies the following Euler-Lagrange equation as follows:

$$\frac{d}{dt}\left(\frac{\partial L}{\partial \dot{y}_k}\right) - \frac{\partial L}{\partial y_k} + \frac{\partial R}{\partial \dot{y}_k} = Q_k, \quad \text{for} \quad y_k = \left[\vartheta(t), s(t), x(t)\right], \quad Q_k = \left[0, 0, F_0\cos\omega t\right], \qquad k = 1\ldots 3, \tag{5}$$

where Q_k is understood to be the reminder of the k-th generalized force when viscous damping of motion of the pendulum body in s direction is accounted for with the Rayleigh dissipation function:

$$R(\dot{\vartheta}, \dot{s}, \dot{x}) = \frac{1}{2} c\left[\frac{d\left(s - l_0\right)}{dt}\right]^2 = \frac{c\dot{s}^2}{2}. \tag{6}$$

After applying the equations (1),(4) and (6) to the Euler-Lagrange equation (5), for each generalized coordinate y_k, we get the three coupled differential equations of motion for each degree of freedom.

1. For the generalized coordinate θ (pendulum angle):

$$s\ddot{\vartheta} + 2\dot{s}\dot{\vartheta} + \ddot{x}\cos\vartheta + g\sin\vartheta = 0. \tag{7}$$

2. For the generalized coordinate *s* (pendulum elongation):

$$m\left(\ddot{s} + \ddot{x}\sin\vartheta - s\dot{\vartheta}^2 - g\cos\vartheta\right) + c\dot{s} + k\left(s - l_0\right) = 0. \tag{8}$$

3. For the generalized coordinate *x* (slider displacement):

$$\left(M + m\right)\ddot{x} + m\cos\vartheta\left(s\ddot{\vartheta} + 2\dot{s}\dot{\vartheta}\right) + m\sin\vartheta\left(\ddot{s} - s\dot{\vartheta}^2\right) = F_0\cos\omega t. \tag{9}$$

Equations (7)-(9) can be algebraically decoupled with respect to the second derivative, thus:

$$\begin{aligned}
\ddot{\vartheta} &= -\frac{1}{s}\left(2\dot{\vartheta}\dot{s} + \rho\cos\vartheta + g\sin\vartheta\right),\\
\ddot{s} &= -\frac{c}{m}\dot{s} - \frac{k}{m}\left(s - l_0\right) + s\dot{\vartheta}^2 - \rho\sin\vartheta + g\cos\vartheta,\\
\ddot{x} &= \rho,
\end{aligned} \tag{10}$$

where $\rho = M^{-1}\left(c\dot{s} + k\left(s - l_0\right)\right)\sin\vartheta + F_0M^{-1}\cos\omega t$ expresses acceleration of the slider.

The system (10) of three second order ordinary differential equations is highly non-linear due to multiplication of state variables and some trigonometric functions. It describes the continuous system dynamics that will be subject to an analysis of long term solutions that will occur far and near its resonance zones. Numerical solution of the system of equations has to be preceded by its transformation to a system of six first order differential equations, assumption of some initial conditions for the six-element state vector and also by the change of the variable $s = \Delta s + \Delta l_{st} + l_0$, so the numerical solution referred to the second degree of freedom (the state variable *s*) will represent an incremental elongation of the spring, i.e., Δs, about its equilibrium length l_0. The system dynamics will be investigated in the next section.

4 RESULTS

In order to solve numerically the system of ordinary differential equations (10), *lsoda* from the FORTRAN library *odepack* is used. Computations are carried out for the following set of system parameters: $M = 5$ kg, $m = 0.3$ kg, $k = 50$ N/m, $c = 10$ (the case of strong damping) and $c = 0.01$ Ns/m (the case of weak damping), $l_0 = 0.35$ m, $F_0 = 4$ N. In Section 4.1, ω was the variable varying in the range of 0-11 rad/s used to investigate the internal and external resonance behavior of the system. Vector of state variables of the system is $\overline{y} = [y_1, \dot{y}_1, y_2, \dot{y}_2, y_3, \dot{y}_3] = [\vartheta, \dot{\vartheta}, \Delta s, \Delta\dot{s}, x, \dot{x}]$.

4.1 Resonance curves for the dynamical system with strong and weak damping effect

Figures 2 and 3 present the resonance curves of the analyzed system that is damped with two coefficients of damping, i.e., $c = 10$ and 0.01 Ns/m, respectively. Zero initial conditions with the high and low damping effect and without any autoparametric internal resonance have been imposed on all state variables. In fact, zero initial condition imposed on the Δs state means, that motion of the pendulum body in *s* direction begins from the length of static elongation of the spring, $\Delta l_{st} + l_0$. Moreover, each maximal amplitude of the system's displacements and rotation was read after 1000 seconds of observation. Omitting a transitory phase of motion a steady-state responses were measured.

In Figure 2, when the excitation acts horizontally on the body of mass *M*, two resonant amplitudes of the states y_1 and y_2, corresponding to angular frequencies $\omega_r = 4.56$ and 4.57 rad/s are observed, respectively. The third component of the system state vector, i.e., the displacement *x* of the slider is not in any resonant state (there not appears any peak of maximal amplitude also in Figure 3, corresponding to almost not existing damping of the system), because for the very small angular frequency of excitation (here, it is the minimum on the vertical axis), the mass *M* moves quickly to the right until the sign of the excitation force amplitude will be changed (in this point, on the third plot in Figures 2 and 3 $max|y_3|$ reaches about 1.55 m for $\omega = 1$ rad/s).

In Figure 3 more peaks is observed due to weak dissipation of energy accumulated in the periodically forced mechanical system. We observe a proper developing of the resonance curve, since its first resonance peak remains a little changed while the new ones between 5.5-6.5 appear. It is very interesting that the slider as a suspension point of the variable-length pendulum does not fall into any resonance state (see red line) even in the weakly damped realization of the mechanical structure.

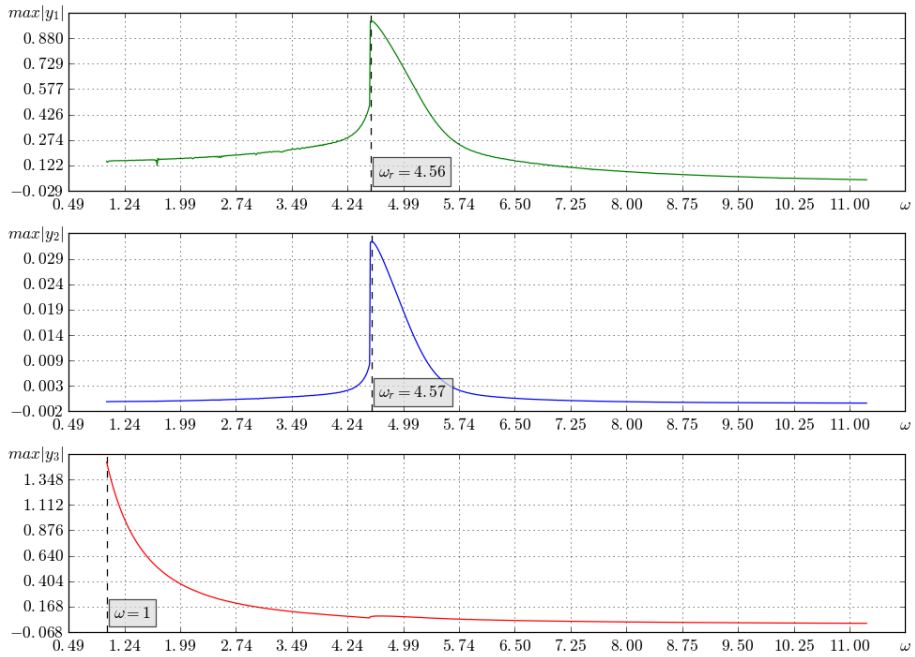

Figure 2: *Resonance curves of the forced spring pendulum system corresponding to maximum absolute values of the state variables $y_1 = \theta$, $y_2 = \Delta s$ and $y_3 = x$. The angular frequency range $\omega \in (1, 11)$ is divided by 1000 samples. Damping of the pendulum $c = 10$ Ns/m. Maximal amplitude frequencies are matched by ω_r.*

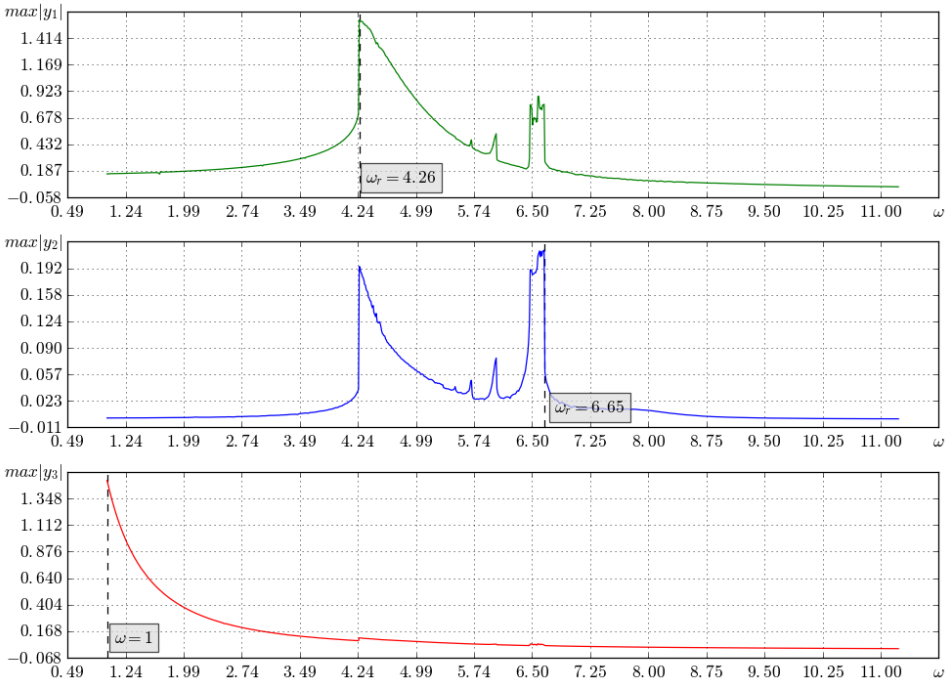

Figure 3: *Resonance curves of the forced variable-length spring pendulum corresponding to maximum absolute values of the state variables $y_1 = \theta$, $y_2 = \Delta s$ and $y_3 = x$. The angular frequency range $\omega \in (1, 11)$ is divided by 1000 samples. Damping of the pendulum $c = 0.01$ Ns/m. Maximal amplitude frequencies are matched by ω_r.*

4.2 Time histories with corresponding power spectral densities

Time histories of the slider-pendulum mechanical system's responses near, and for a relation, exactly at peaks of the resonance amplitudes will be investigated. Power spectral densities of the time histories are estimated numerically using FFT. The strongly damped pendulum is analyzed at the first stage of the investigations, see Figures 4-6, while the dynamics of the very weakly damped pendulum is discussed at the second stage, see Figures 7-9.

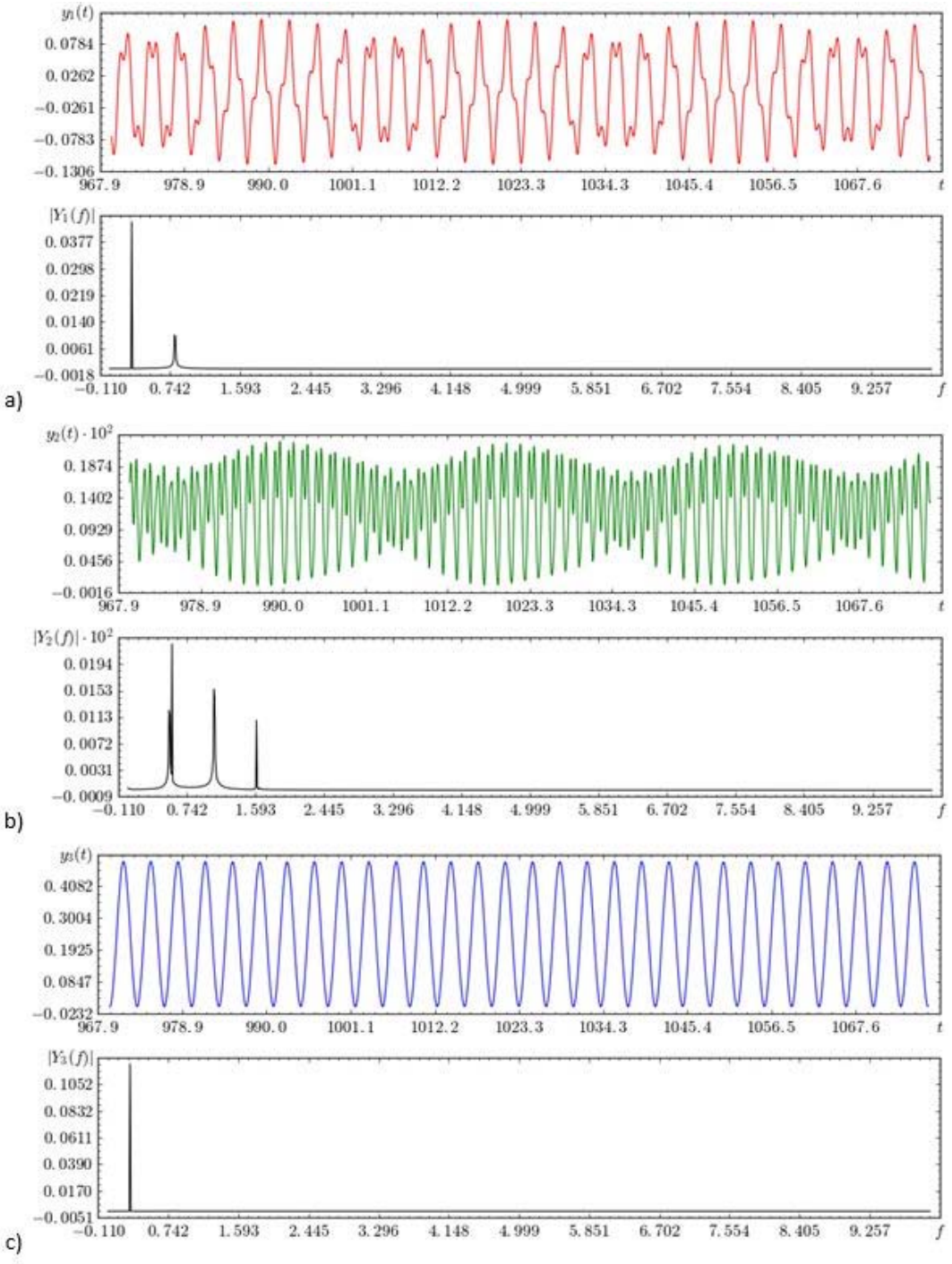

Figure 4: *Time histories with corresponding power spectral densities for the case of strongly damped spring pendulum ($c = 10$ Ns/m). The beginning of observation $t_0 = 969.408$, the end of observation $t_k = 1077.12$ s, the observation time $t_{ob} = 107.712$ s corresponding to $n_T = 30$ periods of excitation force, the slider excitation frequency $\omega = 1.75$ rad/s.*

In Figure 4, the time responses of the pendulum angle (y_1) and the slider displacement (y_3) are synchronized with respect to the first dominant frequency $f_1 \approx 0.2785$ Hz. It is interesting that, in parallel, the pendulum's angular oscillations exhibit also a second dominant frequency at $f_2 \approx 0.7984$ Hz. Elongation Δs of the elastic pendulum oscillates with four frequencies between 0.5 and 1.6 Hz. For the assumed excitation force's angular frequency $\omega = 1.75$ rad/s, the system response is far from the resonance peak shown in Figure 2, since two time histories exhibit some irregular motions. It is observable for the pendulum states $y_1(t)$, $y_2(t)$ and a few frequencies of oscillations reported on the power spectra $|Y_1(f)|$ and $|Y_2(f)|$. As a result of such configuration, the mechanical system forced with the angular frequency $\omega = 4.56$ rad/s oscillates in a purely periodic way, as it is confirmed in Figure 5d by the 1-point Poincaré maps drawn on the corresponding phase planes. Each of the maps drawn with RGB colours consists of n_T overlapping dots. The technique of common visualization of Poincaré maps in relation to their phase planes was introduced in (Awrejcewicz and Olejnik, 2003).

Worth noticing is the fact that with respect to the excitation force's angular frequency $\omega = 4.56$ rad/s, being the one resonant frequency for the strongly damped slider-pendulum system, the maximal amplitudes of angular oscillations of the pendulum, shown in Figure 5a, are nearly nine times larger in comparison to the maximal amplitudes of oscillations shown in Figure 4a ($\omega = 1.75$ rad/s). The presence of resonance in the strongly damped mechanical system is even significant.

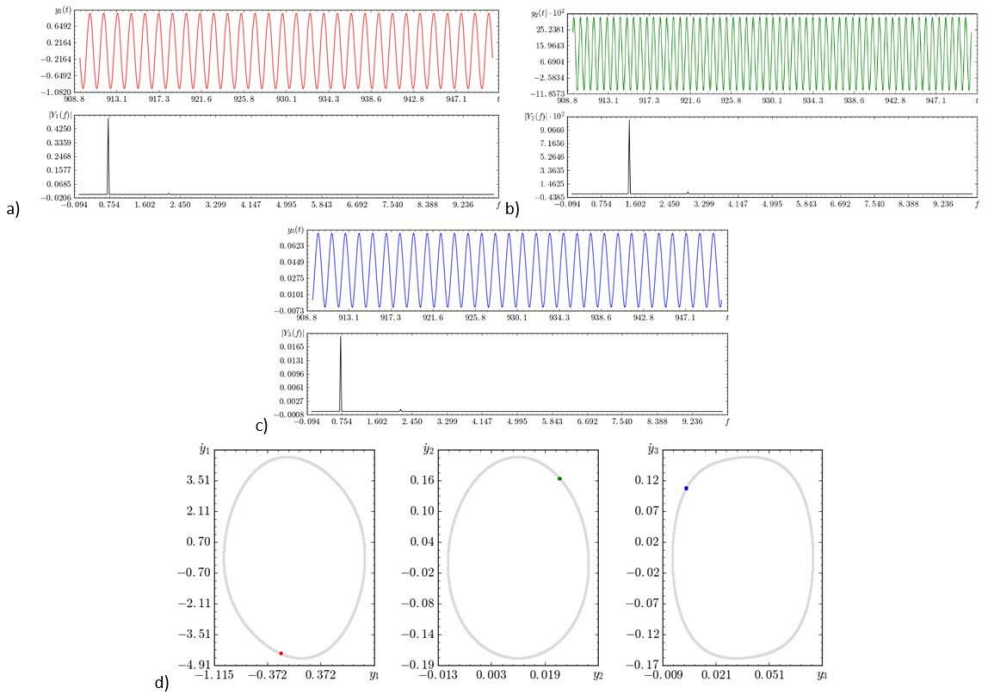

Figure 5: *Time histories of a limit cycles with corresponding power spectral densities, phase planes (gray lines) and Poincaré maps (red, green and blue dots) for the case of strongly damped spring pendulum (c = 10 Ns/m). The beginning of observation $t_0 = 909.414$, the end of observation $t_k = 950.751$, the observation time $t_{ob} = 41.337$ s, corresponding to $n_T = 30$ periods $T = 1.3779$ s of excitation force, the slider excitation frequency $\omega = 4.56$ rad/s.* ***Figure 5:*** *(continued).*

The three-degrees-of-freedom mechanical system's bodies oscillating with two and more dominant frequencies, that in addition, can be mutually separated open the dynamical system's phase space on the onset of multi-periodic or quasi-periodic behaviour. Such dynamics is observed for the solutions shown in Figure 6. Observing the time trajectories longer, the slider will still exhibit 1-periodic motion in the direction y_3, and the Poincaré maps on the $(y_1, \dot{y}_1)$ and $(y_2, \dot{y}_2)$ planes of cross-sections of phase space of the analysed dynamical system will create two closed curves (see Figure 6d), corresponding to amplitude modulated time histories.

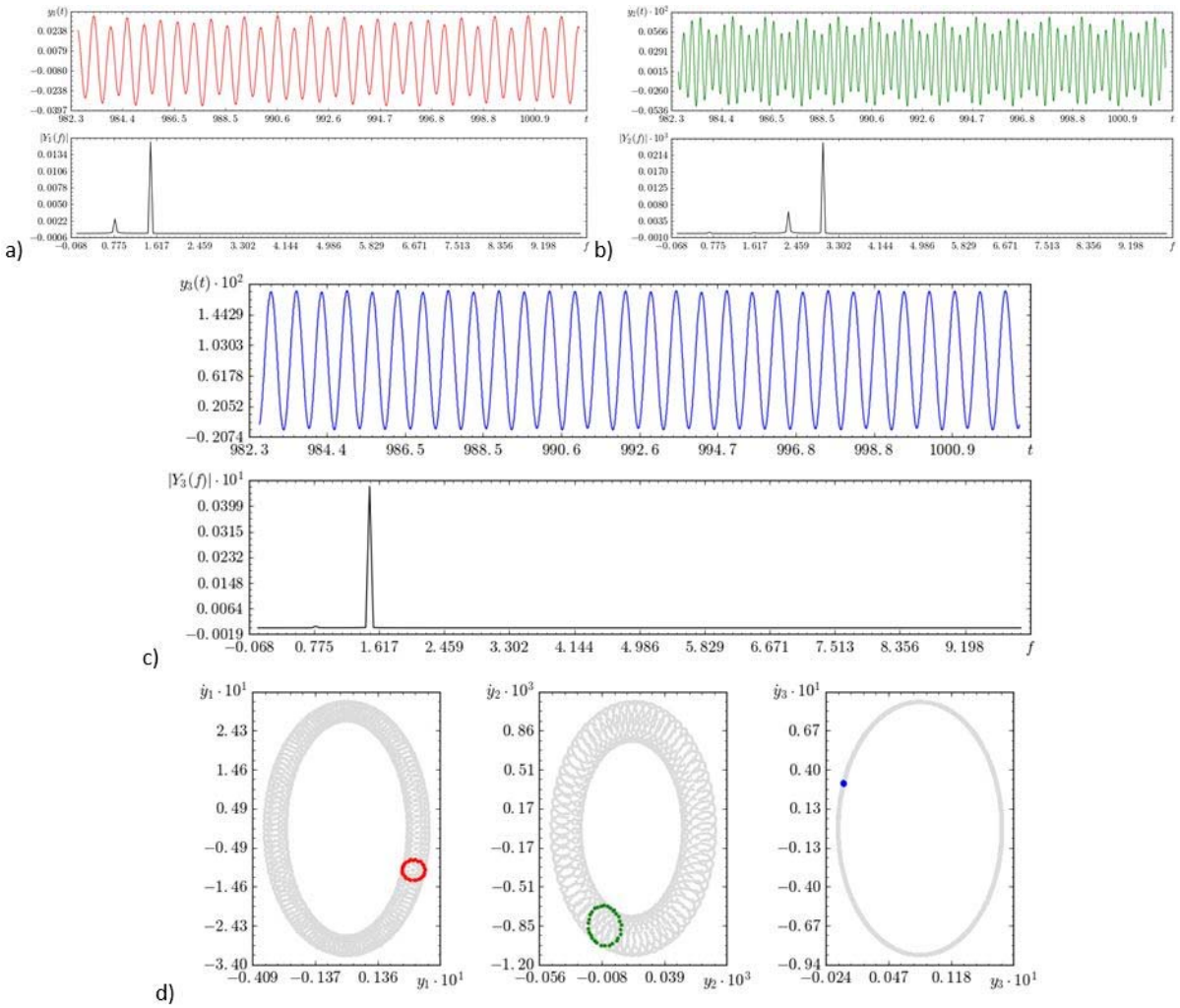

Figure 6: *Time histories with amplitude modulation and corresponding power spectral densities, phase planes (gray lines) and Poincaré maps (red, green and blue dots) for the case of strongly damped variable-length spring pendulum (c = 10 Ns/m). Parameters: t_0 = 982.6215, t_k = 1002.675, t_{ob} = 20.0535, T = 0.66845 s, n_T = 30, ω = 9.4 rad/s.* ***Figure 6:*** *(continued).*

A steady-state quasi-periodic motion of the strongly damped pendulum body and a 1-periodic motion of the slider is achieved. Comparing the power spectra in Figure 6a and c, the frequency of motion of the slider is synchronized with the second dominant frequency of angular oscillations of the pendulum. Elongation Δs of the elastic pendulum oscillates with two frequencies higher than 1.5 Hz.

At the next stage of our study, the dynamics of the very weakly damped pendulum is discussed. In Figure 7, we see an interesting example of quasi-periodic oscillations of the slider-pendulum system in each degree of freedom. It is confirmed in Figure 7d by three closed color curves on Poincaré maps. The slider oscillates quasi-periodically with the frequency $f_2 \approx 0.9707$ being synchronized with the same frequency of angular oscillations of the pendulum. Additionally, with regard to the weakly damped case and in comparison to the previous case, the elongation of the spring pendulum is much greater as well as the remaining state variables take higher maximal amplitudes of oscillations.

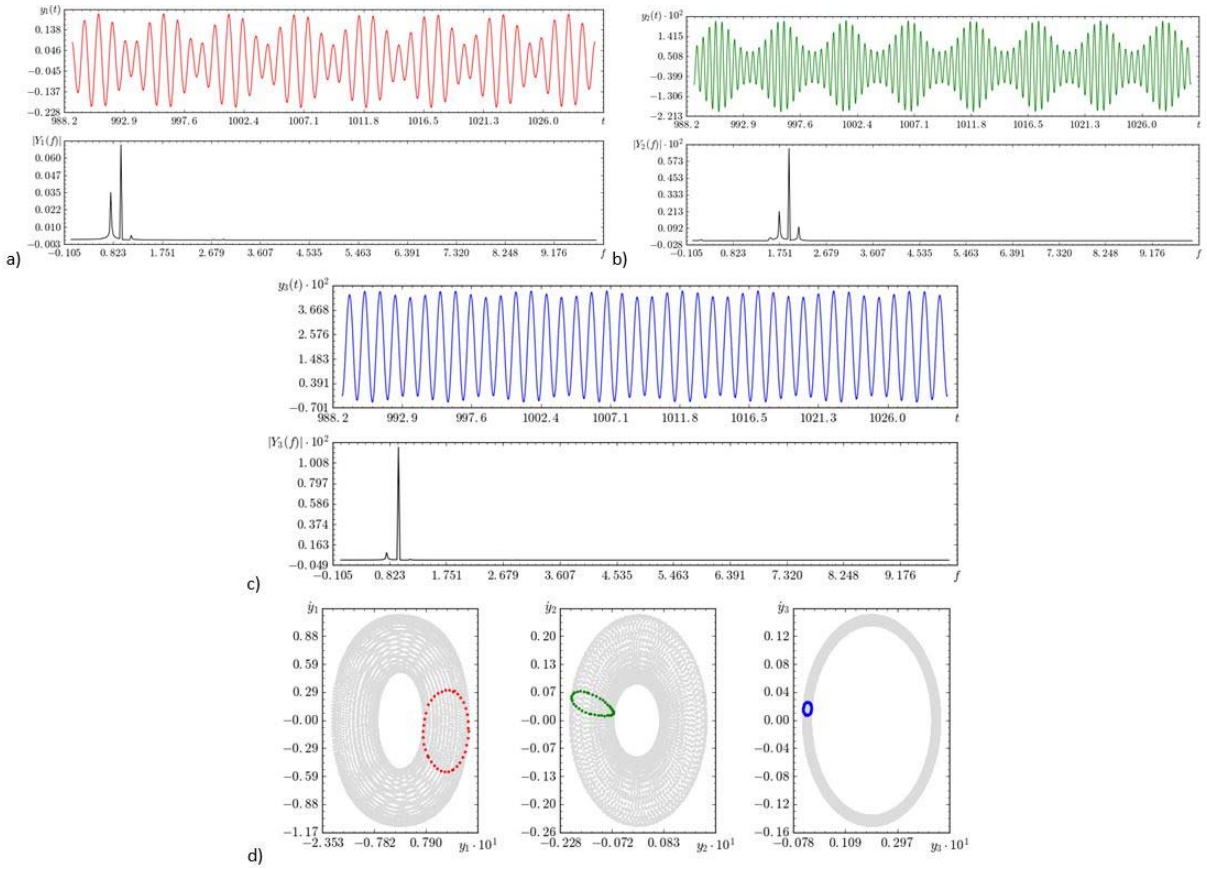

Figure 7: *Time histories with amplitude modulation and corresponding power spectral densities, phase planes (gray lines) and Poincaré maps (red, green and blue dots) for the case of weakly damped variable-length spring pendulum (c = 0.01 Ns/m). Parameters: $t_0 = 988.848$, $t_k = 1030.05$, $t_{ob} = 30.9015$, $T = 1.03005$ s, $n_T = 40$, $\omega = 6.1$ rad/s.*

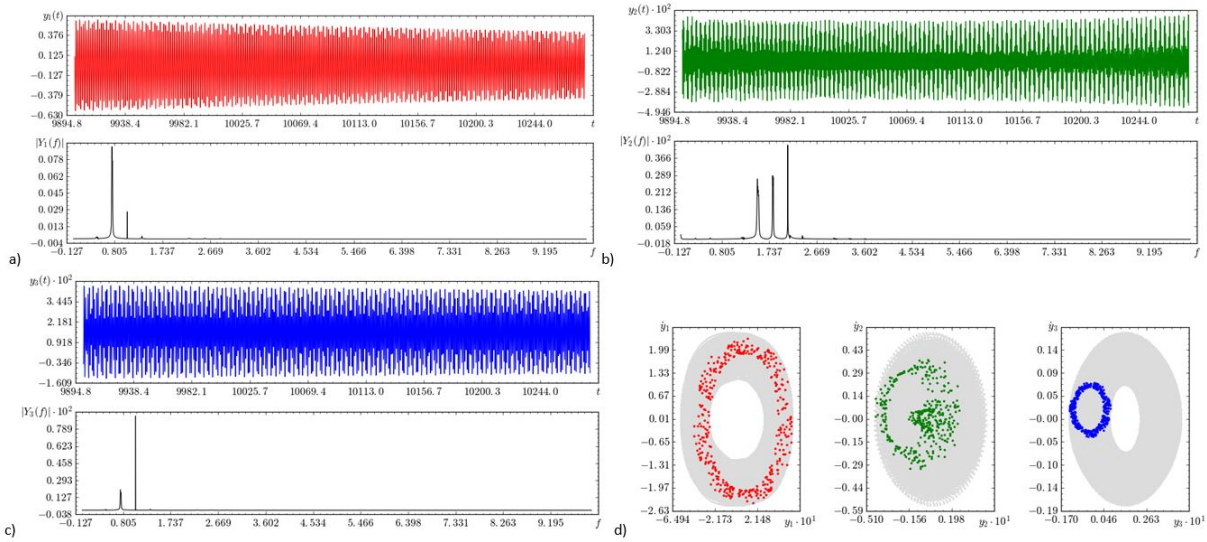

Figure 8: *Time histories of a chaotic solution with corresponding power spectral densities, phase planes (gray lines) and Poincaré maps (red, green and blue dots) for the case of weakly damped variable-length spring pendulum (c = 0.01 Ns/m). Simulation parameters: $t_0 = 9900.8$, $t_k = 10281.6$, $t_{ob} = 380.8$ s, $T = 0.952$ s, $n_T = 400$, $\omega = 6.6$ rad/s.*

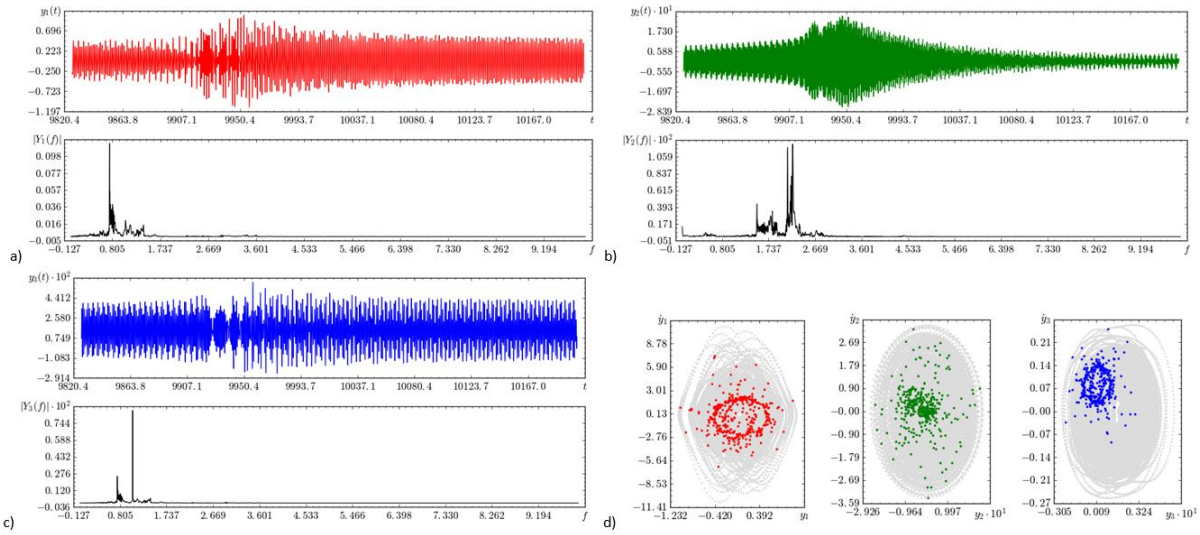

Figure 9: *Time histories of a chaotic solution with corresponding power spectral densities, phase planes (gray lines) and Poincaré maps (red, green and blue dots) for the case of weakly damped variable-length spring pendulum (c = 0.01 Ns/m). Parameters: $t_0 = 9826.44$, $t_k = 10204.38$, $t_{ob} = 377.94$, $T = 0.94485$ s, $n_T = 400$, $\omega = \omega_r = 6.65$ rad/s.*

Figures 8 and 9 present a chaotic dynamics observed at two external excitation frequencies of which the first, $\omega_1 = 6.6$ rad/s, is located in a close neighborhood of the resonance peak and the second one at $\omega_1 = 6.65$ rad/s exactly at this peak (see Figure 3). After a long observation time $t = 9950$ s a sudden elongation of the pendulum length is reported. It is caused by the long lasting resonance state of the whole structure at the excitation frequency ω_r (see Figure 3), producing many resonance frequencies of oscillations shown by the power spectra in Figures 8 and 9.

Let us analyze the spectra of power densities for the weakly damped variable-length pendulum. All the scatter graphs are rugged, but one is able to distinguish a few dominant frequencies of oscillations of each body of the mechanical system in: a) the angular displacement θ of the pendulum, i.e.: $f_{11} \approx 0.7514$, $f_{12} \approx 0.7594$, $f_{13} \approx 0.7700$, $f_{14} \approx 0.8070$; b) the elongation Δs of the pendulum, i.e.: $f_{21} \approx 2.1167$, $f_{22} \approx 2.1961$, $f_{23} \approx 2.2173$; c) the linear displacement x of the slider, i.e.: $f_{31} \approx 0.7514$, $f_{32} \approx 1.0584$. The angular frequency of excitation ω_r at the maximal peak that can be read in Figure 3 is nearly an integer multiple of the frequencies f_{14}, f_{21}, i.e.: $\omega_r/2\pi/f_{14} \approx 12.94 \approx 13$ i $\omega_r/2\pi/f_{21} \approx 4.93 \approx 5$. According to that, the frequencies f_{14}, f_{21} are the resonance frequencies of oscillations of the variable-length spring pendulum in two states: θ and Δs, respectively.

The assumed set of parameters of the oscillator and the external excitation force (see introduction to Section 4) is rather destructive for the investigated mechanical structure. Damping is here very small. Therefore, there exists a minor dissipation of kinetic energy of oscillations in the structure which is transferred all the observation time between its component bodies.

A qualitative assessment of the dynamical behavior both near and exactly at the resonance frequencies of oscillations allows us to draw some conclusions. In the resonance regime, points of Poincaré maps are irregularly distributed on the assumed phase planes (see Figures 8d and 9d), and the investigated dynamical system can unpredictably switch to another range of amplitudes of oscillations in each degree of freedom. One could secure the periodically forced structure from the dynamical presence in any reported resonance zone by a selection of proper angular frequencies of external force acting on it. In contrary to this case, if the periodic excitation is imposed by the external environment and the mechanical structure cannot avoid it, then a change in system parameters like masses of the component bodies or spring stiffness of the variable-length pendulum can be done.

4.3 Poincaré maps of more sophisticates dynamical responses of the system

Previous sections brought us a wider look at dynamical properties of the analyzed mechanical system. In this part of our study we would like to check if the triple oscillator can be a source of chaotic attractors exhibited by all or even not all system states while the other will last on a periodic orbits.

Parameters of the slider-pendulum system remain unchanged, since the frequency of excitation will vary in the examined range taken into consideration in Figure 2 and 3 as well as damping of the pendulum elongation will switch also between the two examined values.

Figure 10a-c presents portraits of a two-, three- and quasi-periodic motion. It is the basic kind of behavior of the analyzed system. Figure 10b and c shows a very frequently observed quasi-periodic motion of the pendulum, and in Figure 10d, a chaotic response of the system oscillating in the resonance is observed. Figure 10c and d confirm that also the slider can oscillate irregularly. In particular, the quasi-periodicity of both pendulum states shown in Figure 10c stands for the internal resonance which is associated with the transmission of energy between the two modes of oscillations.

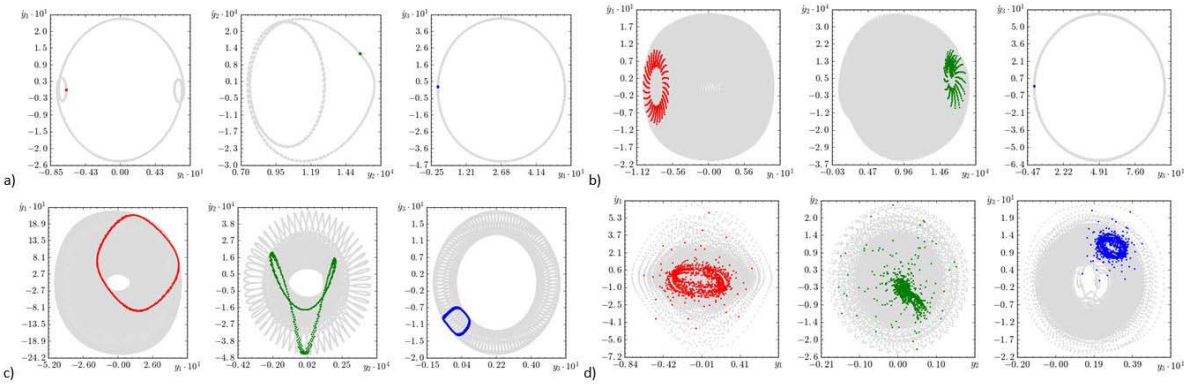

Figure 10: *Poincaré maps on the background of phase planes: a) c = 10 Ns/m, ω = 1.68 rad/s, t_0 = 9350.0, t_k = 11220.0, t_{ob} = 1870.0, T = 3.74 s, n_T = 500; b) c = 10 Ns/m, ω = 1.24 rad/s, t_0 = 2538.6171, t_k = 5077.2342, t_{ob} = 551.15, T = 5.0671, n_T = 501; c) c = 0.01 Ns/m, ω = 5.7 rad/s, t_0 = 9920.7, t_k = 10471.85, t_{ob} = 551.15, T = 1.1023, n_T = 500; d) c = 0.01 Ns/m, ω ≈ ω_r = 6.52 rad/s, t_0 = 14455.5, t_k = 15419.2, t_{ob} = 963.7, T = 0.9637 s, n_T = 1000.*

4.4 Numerical solution

The numerical solution of the continuous system does not require any special methods. It has been obtained with the use of a standard integration procedure. The system of ordinary differential equations was solved using *lsoda* from the FORTRAN library *odepack* with control of the vector of local errors *e* in *x*, according to the inequality of the form: max||e/e_w|| < 1, where $e_w = r_{tol}|x| + a_{tol}$ at the relative and absolute tolerances at each step of integration equal to 1.49012e-8. The integration procedure solves the initial value problem for stiff and non-stiff systems of first order ODEs as follows:

$$\frac{d\overline{x}}{dt} = \overline{f}(\overline{x}, t) \quad \text{at} \quad \overline{x}_0 = \overline{x}(0), \quad t_0 = 0. \tag{11}$$

Due to periodic excitation of the pendulum suspension, the time period of excitation force is assumed in the numerical integration as a multiplicity of the time step (here, 0.00005 s), and then, the horizon of observation t_{ob} included in t_0 to t_k is assumed as multiplicity of the period of excitation. It is to secure proper sampling intervals of the Poincaré maps generated during the simulation, accuracy of solutions of the long term observations as well as most possibly exact repeatability of the periodic forcing of the pendulum slider. Solutions presented in Section 4 are obtained after omitting transition states. Finally, the obtained series of data is stored as tables in files which are imported by a plotting program to draw the solutions.

4 CONCLUSIONS

A mechanical structure consisting of a variable-length pendulum attached to an oscillating suspension was subject to a dynamical analysis. The system dynamics was investigated based on the derivation of mathematical model and the resonance plots obtained for two cases, involving a strong and weak damping of incremental elongation of the pendulum. The observations brought us interesting results, summarizing that the three-degrees-of-freedom mechanical system with partial dissipation of kinetic energy of motion oscillates mainly periodically and quasi-periodically. Nevertheless, the system dynamics exhibited chaos in a close vicinity of resonance peaks of maximum amplitudes. The damped spring pendulum with a moving point of its attachment has two modes of oscillations, the pendulum angle of rotation mode and the spring incremental elongation mode. It has been shown, that the two modes are coupled, and the oscillations energy is transmitted between the two modes. It is interesting, that in some cases, the energy was not transferred to the slider. Figure 10b stands for a good example of such property

of the analyzed mechanical system. The internal resonance is a feature that can make the damped spring pendulum with a slider useful for vibration control of unstable structures.

References

Aduyenko, A.A. and Amel'kin, N.I. (2015). Resonance rotations of a pendulum with a vibrating suspension, Journal of Applied Mathematics and Mechanics, 79(6):531–538.

Awrejcewicz, J. and Olejnik, P. (2003). Stick-slip dynamics of a two-degree-of-freedom system. International Journal of Bifurcation & Chaos, 13(4):843–861.

Hatwal, H., Mallik, A.K. and Ghos A. (1983). Forced nonlinear oscillations of an autoparametric system – Part 2: Chaotic responses, Transactions of the ASME, Journal of Applied Mechanics, 50:663–668.

Kartachov, D. (2016). Pendulum-cart system analysis of the equations of motions, 201-HTL-VA Differential Equations.

Lynch, P. (2002). Resonant motion of the three-dimensional elastic pendulum, International Journal of Non-Linear Mechanics, 37:345–367.

Moon, F.C. (1987). Chaotic Vibrations, John Wiley & Sons, Inc. (New York).

Nayfeh, A.H. and Mook, D.T. (1979). Nonlinear Oscillations, Wiley (New York).

Olejnik, P. and Awrejcewicz, J. (2018). Coupled oscillators in identification of nonlinear damping of a real parametric pendulum, Mechanical Systems and Signal Processing, 98:91–107.

Plaksiy, K.Yu. and Mikhlin, Yu.V. (2017). Interaction of free and forced nonlinear normal modes in two-DOF dissipative systems under resonance conditions, International Journal of Non-Linear Mechanics, 94, 281-291.

Rossikhin, Yu.A. and Shitikova M.V. (2006). Analysis of free non-linear vibrations of a viscoelastic plate under the conditions of different internal resonances, International Journal of Non-Linear Mechanics, 41(2):313–325.

Sado, D. (2003). The Dynamics of a Coupled Three Degree of Freedom Mechanical System, Warsaw University of Technology (Warsaw).

Srinivasan, P. and Sankar, T.S. (1974). Autoparametric self-excitation of a pendulum type elastic oscillator, Journal of Sound and Vibration, 6:549–557.

Zhang, P., Ren, L., Li, H. and Jiang, T. (2015). Control of wind-induced vibration of transmission tower-line system by using a spring pendulum, Mathematical Problems in Engineering (10):1–10.